Ocean Sci. J. (2017) 52(3):345–357
http://dx.doi.org/10.1007/s12601-017-0021-8

Article

Available online at http://link.springer.com
SpringerLink

Ocean Science Journal
pISSN 1738-5261
eISSN 2005-7172

Fossil Diatom Assemblages as Paleoecological Indicators of Paleo-water Environmental Change in the Ulleung Basin, East Sea, Republic of Korea

Suk Min Yun[1,4,5], Taehee Lee[2], Seung Won Jung[1], Joon Sang Park[3], and Jin Hwan Lee[4]*

[1]*Library of Marine Samples, South Sea Research Institute, KIOST, Geoje 53201, Korea*
[2]*Jeju Environment Research Section, Jeju International Marine Science Research & Logistics Center, KIOST, Jeju 63349, Korea*
[3]*Marine Ecosystem and Biological Research Center, KIOST, Ansan 15627, Korea*
[4]*Department of Biology, Sangmyung University, Seoul 03015, Korea*
[5]*Protist Resources Research Division, Nakdonggang National Institute of Biological Resources, Sangju 37242, Korea*

Received 18 February 2016; Revised 28 September 2016; Accepted 28 February 2017
© KSO, KIOST and Springer 2017

Abstract – The fossil diatom assemblage record from two sediment cores obtained from the Ulleung Basin, East Sea, Republic of Korea, revealed changes in the diatom assemblage zones in PG1 and PD3 core samples. The two sediment cores were δC^{14} dated and approximately represented the late Pleistocene–Holocene. The analysis of age zones in the PG1 core and PD3 core was assessed based on the frequency of variations, and occurrences of biostratigraphical fossil diatom species. During the Last Glacial Maximum (LGM), the sea level was lower than that at present and the Ulleung Basin became isolated from the Pacific Ocean. As a result, there would have been a limited Tsushima Warm Current (TWC) influence, and salinity would have decreased resulting in increased freshwater and coastal diatoms. The distribution pattern of diatoms presented in the cores was associated with changes in water temperature and salinity and the adding of terrigenous material brought about by the input of freshwater. Changes in the abundance of a tychopelagic diatom, *Paralia sulcata,* reflected the effect of the water currents. Diatom temperature (Td) values and the ratio of centric/pennate diatoms provided evidence of limited influences of the TWC and freshwater inflow. It is thought that all assemblage zones were influenced by the TWC, which had an important effect on the distribution and composition of fossil diatoms.

Keywords – freshwater, fossil diatom, Last Glacial Maximum, Tsushima Warm Current, Ulleung Basin

1. Introduction

Marine sediment cores are a fundamental source of data regarding geological history and paleoclimatic changes (Rothwell and Rack 2006); therefore, it is necessary to recover useful paleoenvironmental data (Haschke 2006). Diatoms are the dominant marine primary producers and play an important role in the carbon, silica, and nutrient budgets of the ocean (Gebühr et al. 2009). In particular, they are sensitive to changes in physical and chemical conditions. Fossil diatoms are created through a process of sedimentation and fossilization of planktonic diatoms. They are particularly suitable for paleontological studies and have been used widely as paleoenvironmental indicators, including species compositions and relative abundance of the main indicator taxa (Reid et al. 1995). Thus, fossil diatoms provide a valuable tool for studying water quality and reconstructing past environments both in freshwater (e.g., Marciniak 1981; Flower et al. 1997; Witoñ and Witkowski 2003) and marine (e.g., Witkowski 1994; Andreen et al. 2000) ecosystems.

The East Sea is located in the Pacific Northwest, between the Asian continent and the waters around Japan. The East Sea surrounding Korea is more than 2,000 m deep, owing to the topography of the seabed North of the Japan Basin, East of the Yamato Basin, and in the western Ulleung Basin. The Ulleung Basin is a deep, bowl-shaped, back-arc basin bound by the steep continental slope of the eastern Korean Peninsula (Lee and Suk 1998), and it was formed by an extension of the continental crust, accompanied by a progressive southward drift of the Japanese Arc during the late Oligocene to early Miocene (Yoon and Chough 1995). The modern oceanography of the Ulleung Basin is largely affected by the Tsushima Warm Current (TWC) in the Kuroshio Current (western boundary current). The warm-water and high salinity of the TWC is a

*Corresponding author. E-mail: jhlee@smu.ac.kr

major source of the surface water supplied to the southern East Sea (e.g., Moriyasu 1972; Park et al. 2000). However, the surface water of the Ulleung Basin is cold with a low salinity resulting from the Oyashio Cold Current, originating in the Bering and Okhotsk Seas (Yasuda et al. 1996; Ryu et al. 2005). Surface sediments in the southern Ulleung Basin are covered by fine clay, derived mostly from the Nakdong River in Korea and Yangtze River (Changjiang) in China (Cha et al. 2007;

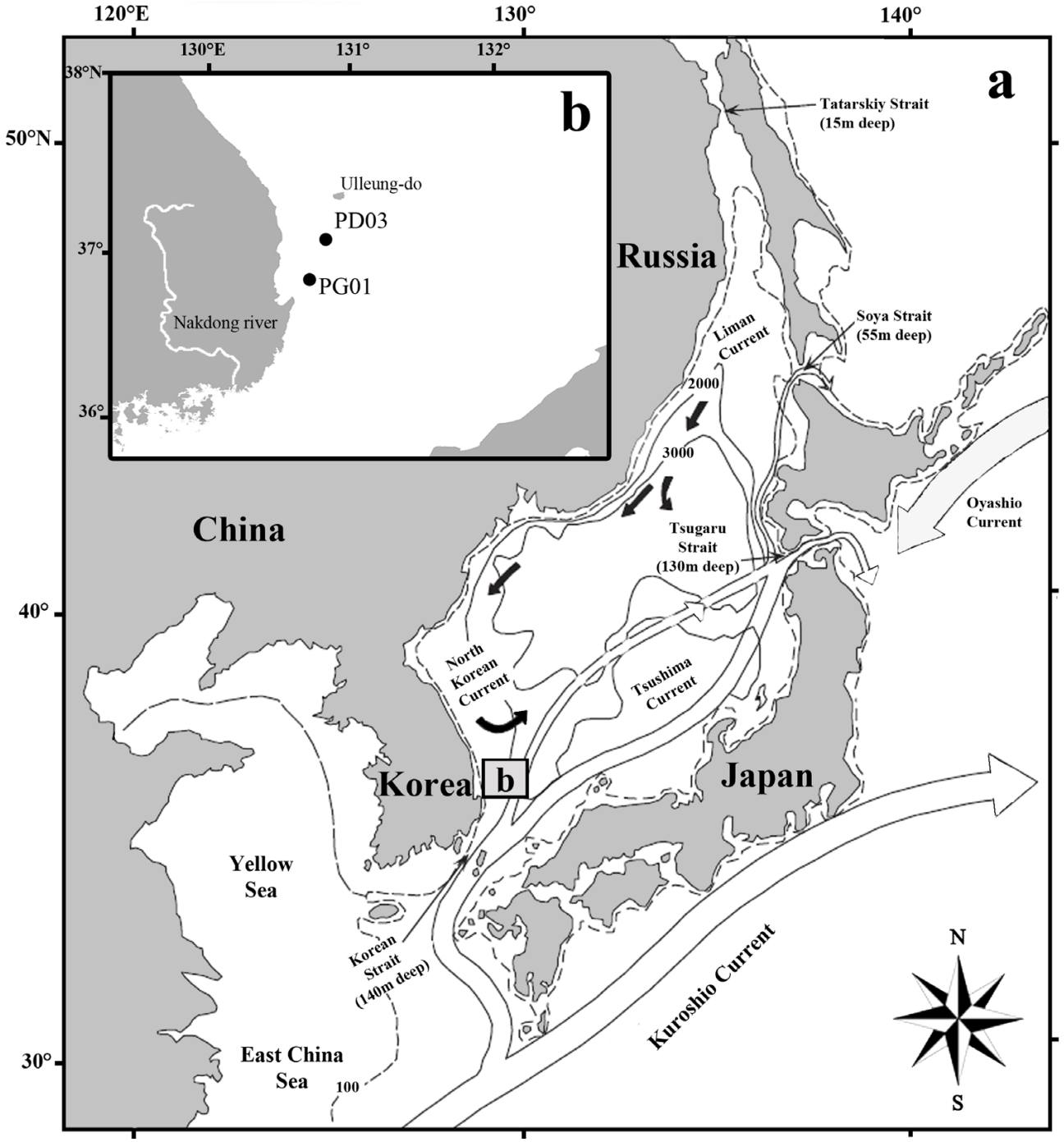

Fig. 1. Maps of the study area. **a:** Location map showing the study area (square box) in the Ulleung Basin, East Sea with simplified dominant currents (modified from Ryu et al. 2005). The Tsushima Warm Current (white arrow) indicates a high salinity, warm current originating from the equatorial region of the western Pacific Ocean. The Oyashio Cold Current (gray closed arrow) represents a low salinity, cold current from the Bering Sea. A black closed arrow indicates a cold long-shore current along eastern Russia and the Korean Peninsula. **b:** Inset figure shows the sites of piston cores PG1 and PD3 in the Ulleung Basin, East Sea

Lim et al. 2011). However, the paleoenvironmental conditions of the Ulleung Basin, such as current inflow, current circulation, sea level fluctuations, and climate change, changed dramatically during the late Pleistocene to Holocene (Oda et al. 1991). Several paleoceanographic studies have discussed the effect of current inflow during and since the last glacial period in the region (Oba et al. 1991; Ujiié et al. 1991, 2003; Xu and Oda 1999; Jian et al. 2000; Lim et al. 2006); however, these studies are limited to the historical effect of current and sea level fluctuations. The objective of the present study is to interpret the paleoenvironments of the Ulleung Basin of South Korea during the late Pleistocene and Holocene based on changes in fossil diatoms and geochemical factors from two sediment cores, PG1 and PD3.

2. Material and Methods

Collected core samples, geochemical factor, and age analysis

Two sediment cores were collected using a piston core during a cruise of r/v "Eardo" organized by the Korea Institute of Ocean Science and Technology (KIOST), in July 2012 (Fig. 1, Table 1). Core PG1 (length of 3.95 m) was taken from the outer part of the Ulleung Basin at a water depth of 1,445 m, whereas core PD3 (length of 3.46 m) was collected outside Ulleung Basin at a water depth of 2,190 m.

Total nitrogen (TN), Total carbon (TC), and Total organic carbon (TOC) contents of the powdered sediments were measured using a Carlo Erba Elemental Analyzer 1108 (CE Instruments, Milan, Italy). The C:N ratio is calculated by the weight ratio of total organic carbon to total nitrogen. Total inorganic carbon contents were measured using a carbon dioxide coulometer (model CM 5014; UIC Inc., Illinois, USA). Total inorganic carbon contents were converted to calcium carbonate ($CaCO_3$) content as a weight percentage using a multiplication factor. The carbonate content was calculated using the equation: $CaCO_3$ (%) = (TC–TOC) × 8.333 (Stein et al. 1994).

Accelerator mass spectrometry (AMS) ^{14}C dating was used on mixed foraminifer species selected from the two cores. Selected carbon samples were dated by Beta Analytic Inc. (Miami, FL, USA). In Fig. 2, AMS ^{14}C ages are listed together with the photographs of the two cores and characteristic layers. All dates were calculated using the Libby half-life of 5,568 years and a reference of 1950 A.D.

Fossil diatom analysis

All of the core samples collected at 10 cm intervals (38 samples in PG1, 36 samples in PD3) weighed approximately 2 g. Collected samples were prepared using the following method (Battarbee 1986): 1 g dry sediment was treated with 10 mL 10% HCl and 50 mL 30% H_2O_2 to remove the calcareous and organic matters. The residue was washed repeatedly with distilled water until clean. The fossil diatoms were quantitatively analyzed using a light microscope (LM, Axio Imager A2, Carl Zeiss, Jena, Germany) at a magnification of × 400 or 1,000. A total of 4,000 cells diatom frustules were counted in each sample (excluding resting spores). Diatom fine structure was observed using a scanning electron microscope (SEM, JEOL, JSM-7600F, Tokyo, Japan) on a prepared sample. The dominant species selected in the fossil diatom samples appeared in high percentages (> 2%) in the core sediment samples. Fossil diatom diversity was calculated using a Shannon's H′ Index (Shannon and Weaver 1949).

Td values and C:P diatom ratio

Td (diatom temperature) values proposed by Kanaya and Koizumi (1966) have been adopted in this study. The Td value is defined as Td = Tw / (Tw + Tc). 'Tw' is the number of warm-water species and 'Tc' is the number of cold-water species. The Td value ranged from 0 to 1: Td values 0.5–1, warm biofacies; Td values 0.2–0.5, temperate biofacies; and Td values 0.0–0.2, cold biofacies. Temperate to warm- and cold-water species used for Td analyses have been provided in Appendix Table 1.

The centric:pennate ratio (C:P ratio), which is the ratio of the number of the centric (usually planktonic species) to pennate (usually benthic species) diatoms, can be useful as an indicator of the relative availability of planktonic and benthic habitats (Cooper 1995a, 1995b).

Table 1. Information of location

Core code	Collection date	Collection depth (m)	Core length (m)	Latitude (N)	Longitude (E)
PG1	Jul. 2012	1445	3.95	36°05'54.8"	130°05'02.0"
PD3	Jul. 2012	2190	3.46	36°59'52.8"	130°59'30.0"

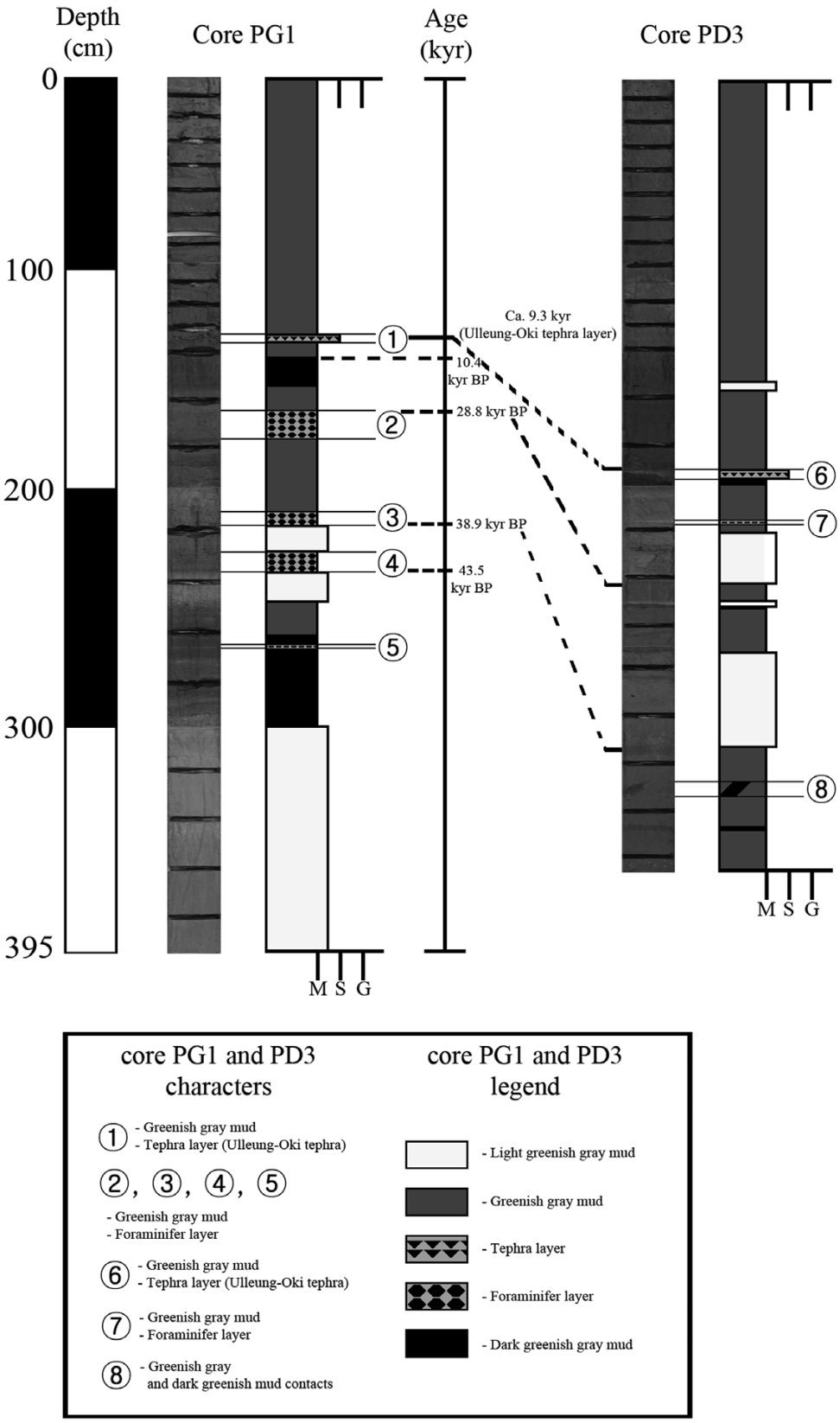

Fig. 2. Photographs of two cores (PG1 and PD3) showing the representative core sediment section, including Ulleung Basin, and characteristic layers (M: mud; S: sand; G: gravel)

3. Results

Core profile and fossil diatoms in core sediments

Core PG1 mostly consisted of greenish-gray and dark greenish-gray mud. The 160–200 and 267–286 cm in the lower part of the core was mixed dark greenish-gray and greenish-gray mud. The 300–395 cm depth consisted of light greenish-gray mud. Core PD3 also mostly contained a distinct dark greenish-gray mud layer. The 310–346 cm depth consisted of greenish-gray sediment. However, we confirmed that 326–328 cm depth was dark greenish-gray mud.

Total fossil diatom abundance of PG1 and PD3 cores ranged from 1.1×10^4 to 3.9×10^4 and 1.3×10^4 to 4.1×10^4 cells/g, respectively (Fig. 3). In core PG1, the highest diatom concentrations were at 2–4 and 102–104 cm, and the lowest diatom concentrations were at 152–154 and 252–254 cm (Fig. 3). In core PD3, the highest diatom concentrations were at 72–74 and 162–164 cm, and the lowest diatom concentrations were at 252–254 cm (Fig. 3). A total of 78 diatom species (43 centric and 35 pennate diatom species) in PG1 and 80 diatom species (47 centric and 33 pennate diatom species) in PD3 were identified and their frequency was expressed as an individual. Centric diatom species dominated the two sites. The number of species present in PG1 and PD3 were 11 (at 252–254 cm) to 33 (at 32–34 cm) and 16 (at 252–254 cm) to 36 (at 72–74 cm), respectively. The number of species increased toward the top. Diatom species diversity ranged from 1.8 to 3.2 in PG1 and 2.0 to 3.1 in PD3. Diversity of diatom taxa was high in the PD3, and the fossil diatoms were well preserved.

Change of fossil diatom composition according to the age zone

Radiometric age was analyzed using foraminifera in core sediments, and the relative ages were inferred by calculating the absolute age of the tephra layer (113–115 cm depth in PG1, 171.5–174 cm depth in PD3). The age results are as follows: in the PG1 core, sections at depths of 132–134, 156–158, 212–214, and 246–248 cm indicated 10.4, 28.8, 38.9, and 43.5 kyr BP, respectively. In the PD3 core, sections at depths of 252–254 and 313–315 cm indicated 28.8 and 38.9 kyr BP, respectively (Fig. 3). Sedimentation rates in PG1 were greater than those in PD3. These results were confirmed by the shallower water depth of PG1 than of PD3. The sedimentary sequences of PG1 and PD3 showed continuous Late Pleistocene, Last Glacial Maximum (LGM), and Holocene records (Figs. 6 and 7).

Three-age zones were established from the whole section of the PG1 and PD3 core (Fig. 3). The Late Pleistocene zone (373–162 cm, approximately 126–11.7 kyr) of the core PG1, was characterized by the dominance of *Paralia sulcata*, *Coscinodiscus asteromphalus*, and *C. centralis*, with the lowest abundance, and slightly lower number of species and species diversity than other age zones. *Navicula directa* occurred at a relatively high abundance (approximately 10.0% at 182–194 cm depth). In addition, freshwater species (e.g., *Cyclotella* spp.) and *Thalassionema frauenfeldii* showed a relatively higher abundance than the other age zones. The LGM zone (154–142 cm, approximately 26.5–14.6 kyr) was dominated by the *P. sulcata, C. asteromphalus*, *C. centralis,* and *Thalassiosira mala*. However, frequencies of *P. sulcata* decreased in the Late Pleistocene zone when other species increased. In this zone, the abundance appeared to increase and the number of species and species diversity decreased slightly in comparison to the Late Pleistocene zone. Since during the Last Glacial Maximum much of the world was cold and dry with frequent storms and a dust-laden atmosphere, this period was not suitable for life in aquatic environments. The Holocene zone (134–2 cm, approximately 11.7 kyr–present) showed a sharp increase in abundance, number of species, and species diversity, but was characterized by relatively low frequencies of *P. sulcata* (4.3% at 11–13 cm depth) as well as a decrease in the number of Thalassiosira, and was characterized by relatively high frequencies of *Actinocyclus octonarius* (10.9% at 62–64 cm depth, 12.0% at 32–34 cm depth and 17.1% at 2–4 cm depth) and *Th. frauenfeldii* (13.3% at 82–84 cm depth).

In the Late Pleistocene zone (346–252 cm) of the core PD3, diatom abundance, number of species, and species diversity were not different from those in the LGM zones, and this zone was characterized by relatively higher frequencies of *P. sulcata* (up to 50.1%). At a depth of 313–315 cm, *Navicula* spp. (up to 6.3%) was abundant, but was generally small in size and poorly preserved. In addition, *Thalassiosira curviseriata* was abundant at 252–254 cm depths (10%). The LGM zone (252–182 cm) had lower abundance, number of species, and species diversity than Holocene zones, and was dominated by relatively high frequencies of *P. sulcata* (up to 34.7%). However, frequencies of *P. sulcata* decreased more abruptly than in the Late Pleistocene zone, and other dominant species increased. This zone was characterized by the dominance of benthic diatoms, including *Th. frauenfeldii* (1.7–7.5%) and *Th.*

nitzschioides (2.9–10.9%). The Holocene zone (182–2 cm) showed the highest abundance, number of species, and species diversity. *P. sulcata* was the dominant species, and its abundance peaked at depths of 172–174 cm (43.4%). Moreover, this zone was characterized by relatively high frequencies of *C. centralis* (10.7% at 62–64 cm depth and 10.7–13.2% at 34–3 cm depth) and *Th. nitzschioides* (9.1–13.3% at 154–132 cm depth).

Diatom temperature (Td values) and centric:pennate (C:P) diatom ratios in Ulleung Basin

Temperate- to warm- and coldwater species used for the Td analysis are included in Supplemental Table 1. The Td values generally increased upwards in PG1 (Fig. 3). The Td value ranged from 0.2 to 1.0, increasing in the 91–93, 132–134, 152–154, and 272–274 cm intervals; whereas at the 111–113, 351–353, and 361–363 cm intervals the Td values decreased abruptly owing to the decrease in warmwater species (e.g., *C. centralis, T. mala*, and *Th. frauenfeldii*). In PD3, Td values also generally increased upwards, and ranged from 0.5 to 1.0; they increased at the 12–14, 62–64, 122–124, and 162–164 cm depths, and, were lowest at the 273–275 cm interval owing to abundance of coldwater species (e.g., *A. curvatulus*).

In PG1, the average C:P ratio ranged from 2.1 to 15.7 (Fig. 3). In PD3, the C:P ratio ranged from 1.7 to 15.1. The C:P ratio increased significantly in the two cores, with dramatic changes in 122–142, 72–74 cm of PG1, and 72–74 cm in PD3, respectively (Fig. 3). The ratio decreased reaching a minimum at 11–13 cm in PG1. The minimum was recorded at 242–244 cm in PD3.

Geochemical factors

TC of PG1 and PD3 ranged from 1.2 to 5.7% and 0.8 to 3.9%, respectively (Fig. 3). TOC of PG1 and PD3 ranged from 1.1 to 3.9% and 0.7 to 3.3%, respectively. TN of PG1 and PD3 ranged from 0.1 to 0.5% and 0.1 to 0.4%, respectively. $CaCO_3$ of PG1 and PD3 ranged from 0.1 to 18.6% and 0.1 to 14.4%, respectively (Fig. 3). In PG1, TC, TOC, and TN contents showed wide fluctuations, particularly below a core depth of approximately 240 cm. $CaCO_3$ contents peaked at 240 cm (18.5%). In PD3, TC, TOC, and TN contents peaked at 180 cm and steadily decreased from the 180 to 30 cm layer. $CaCO_3$ contents peaked at 200 cm depths (14.4%), and decrease towards the surface. C:N ratios of PG1 and PD3 ranged from 7.2 to 10.1 and 4.4 to 8.6, respectively.

4. Discussion

The Ulleung Basin in the East Sea was possibly characterized by low sea surface salinity during the LGM. The low sea surface salinity is affected by large amounts of freshwater input (Tada 1999) from the adjacent river systems (e.g., Yellow, Nakdong, and Seomjin Rivers) (Oba et al. 1991; Park et al. 2000; Lee and Nam 2003, 2004). The sea level drop during the last glacial period exposed most parts of the Yellow Sea, and the coastline moved southward, shifting the Yellow River mouth (Oba et al. 1991; Tada 1999). Freshwater from the Yellow River might have flowed into the East Sea via the Korea Strait. As a result, this water could have mixed with the paleo-Tsushima Current and freshwater derived from the adjacent river systems during the LGM (Oba et al. 1991; Park et al. 2000; Lee and Nam 2003).

In the present study, the dominant species was *P. sulcata*. *Paralia sulcata* is very useful for inferring past aquatic conditions, because it is tychoplanktonic with abundant populations and a cosmopolitan distribution, and is more resistant to dissolution than other diatom species. *Paralia sulcata* is a widely distributed diatom in fossil marine sediments (Zong 1997; Ryu et al. 2005, 2008). This species was first recorded in the late Cretaceous (Girard et al. 2009) and provides the oldest diatom fossil record in the present study. *Paralia sulcata* prefers a low-salinity environment, low light (Blasco et al. 1980), warm water, upwelling (Lange et al. 1998), and is especially abundant in fine-grained, organic rich sediments (Zong 1997). According to Zong (1997), the high abundance of *P. sulcata* in basins (e.g., Ulleung Basin) reflects its ability to adapt to particular environmental and depositional conditions, including greatly varied salinity and fine-grained and organic-enriched sediment. Under these conditions, *P. sulcata* seems more competitive than many other marine or brackishwater species. During the LGM, the variation in abundance of this species may have been due to sea level changes. After the LGM, this species was affected by the water currents. These environmental changes can be confirmed by the C:P ratio and Td value. C:P ratios can be useful as indicators (Cooper 1995a, 1995b) and an index of trophic condition supporting earlier findings of Nyagaard (1949). C:P ratios in PG1 cores were higher than those in PD3 cores in all ages. These results obviously indicate a relatively steady relationship between pennate and centric diatom populations in the Ulleung Basin. Environmental changes that could increase C:P ratios include blooms of centric diatoms, larger populations, or increased levels of

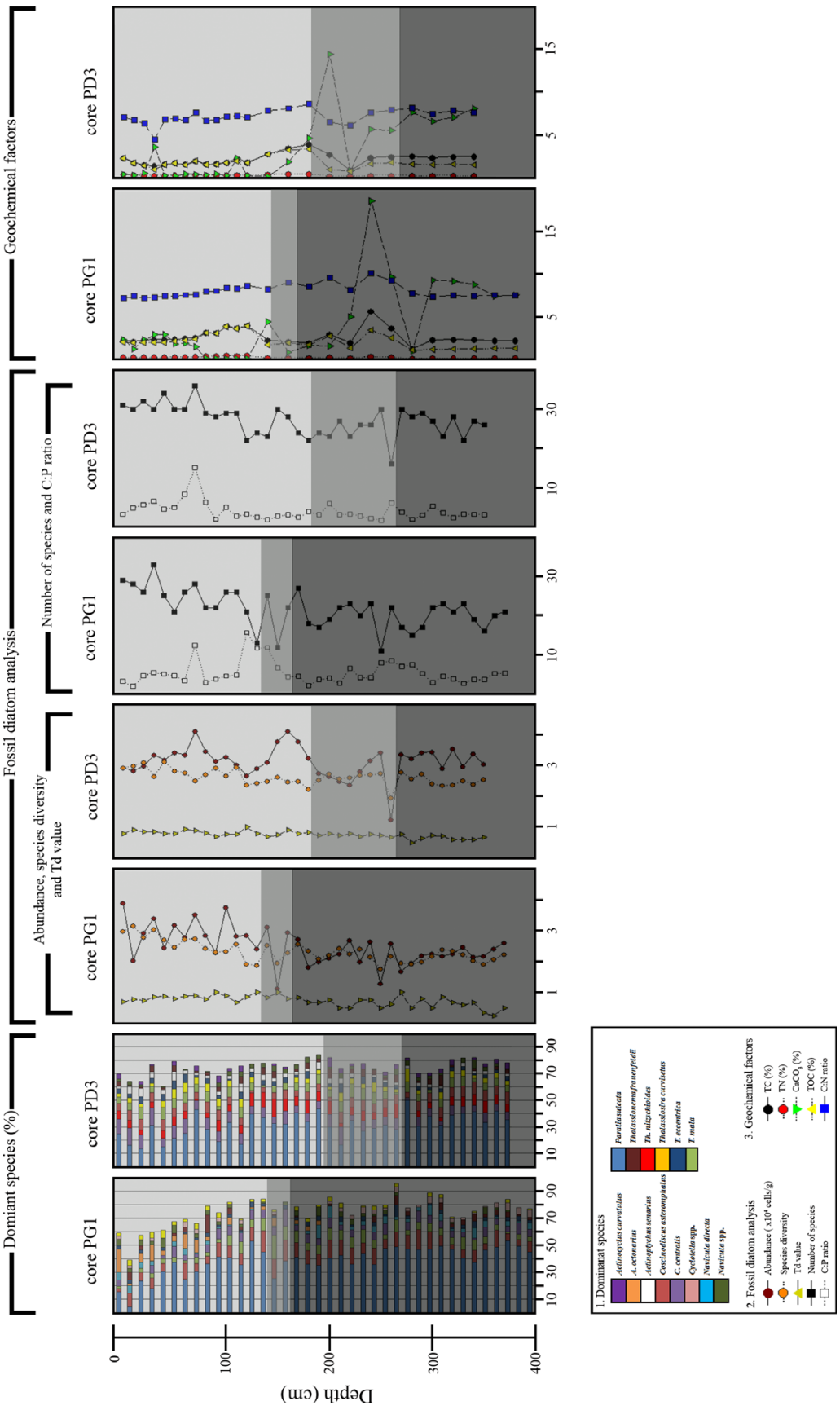

Fig. 3. Downcore variation of fossil diatom community and geochemical factors according to the age zone. The dark grey, grey and light grey colors represent the Late Pleistocene, Last Glacial Maximum, and Holocene zone, respectively. TC: total carbon (%); TN: total nitrogen (%); $CaCO_3$: calcium carbonate (%); TOC: total organic carbon (%)

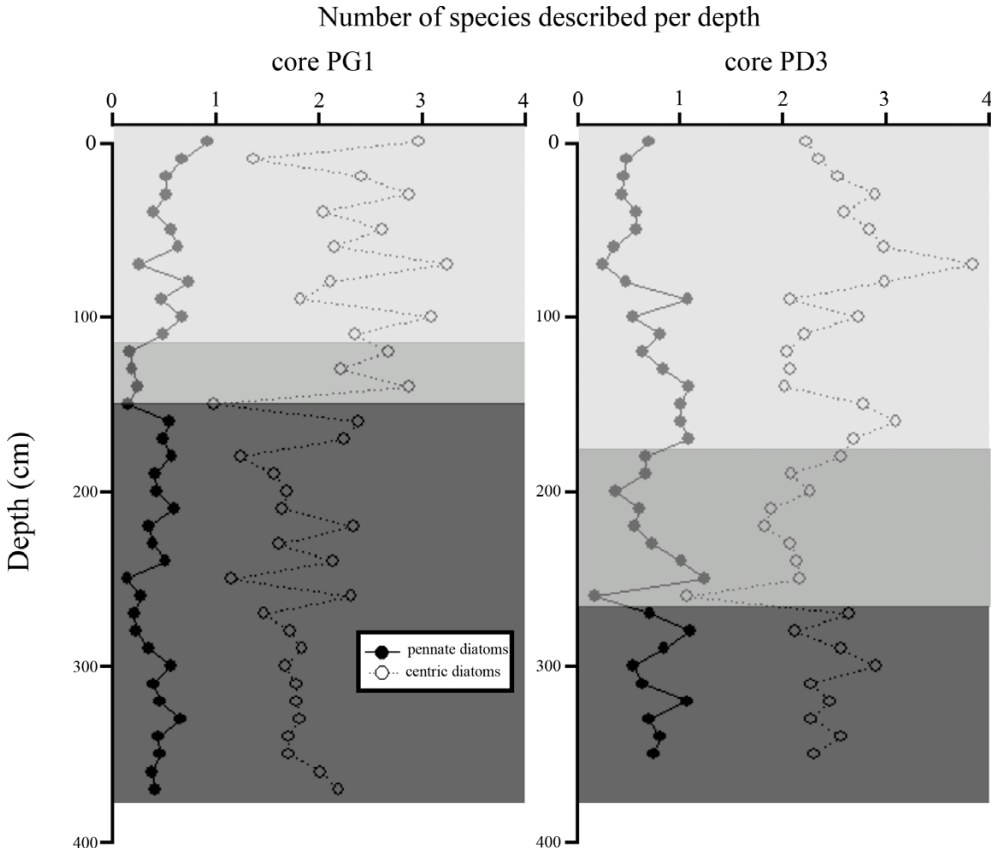

Fig. 4. Downcore changes in number of species between centric and pennate diatoms (PG1 and PD3 cores). The dark grey, grey and light grey colors represent the Late Pleistocene, Last Glacial Maximum, and Holocene zone, respectively

suspended sediment, all of which would increase turbidity and reduce light availability to the pennate diatom species (Pyle et al. 1998). In the present study, the population of centric diatoms was higher than that of pennate diatoms (Fig. 4). These results are attributed to environmental differences in PG1 and PD3 cores. PG1 was located 62 km from the coast, whereas PD3 was located approximately 141 km from the coast in Korea. As mentioned previously, during the LGM, a lowered sea level was enough to close the East Sea. As a result, current influx would have been limited. However, freshwater input increased from adjacent rivers of the surrounding lands (Ryu et al. 2005). The salinity decreased and freshwater species (e.g., *Cyclotella* spp.) or low salinity coastal water diatoms, such as *P. sulcata*, increased. In the present study, the relative abundance of *P. sulcata* in PG1 was higher than in PD3 (Figs. 5 and 6). In addition, freshwater species such as *Cyclotella* spp., were more abundant in PG1 than PD3 (Figs. 5 and 6). These species are found frequently in sediments of upwelling zones (Schuette and Schrader 1979; Lange et al. 1998; Ryu et al. 2005). In general, productivity in the upwelling zones is high, where low productivity is related to the weak and more discontinuous effects of upwelling (Ryu 2005). In such upwelling regions on the continental slope, species distribution is defined by the constant presence of neritic assemblages in areas close to the coast (Ryu 2005). As a result, diversity in fossil diatom assemblages, and the presence or absence of certain fossil diatoms can be used to distinguish conditions of strong and permanent upwelling from conditions of occasional upwelling and production from river discharge (Abrantes 1991). These changes are possibly due to the fluctuation of nutrient availability by current influx, sediment flow, and location in collected cores. Fluctuation of geochemical factors (TC, TN, $CaCO_3$, TOC, C:N ratio) are possibly owing to nutrient availability, determined by current influx, sediment flow, and location of collected cores. All geochemical factors increased upward in the collected cores. The values of the geochemical variables for PG1 and PD3 during the last interglacial and after the LGM periods were higher than those during the LGM. All geochemical factors showed higher values in core PG1 than in the other core. These results indicate

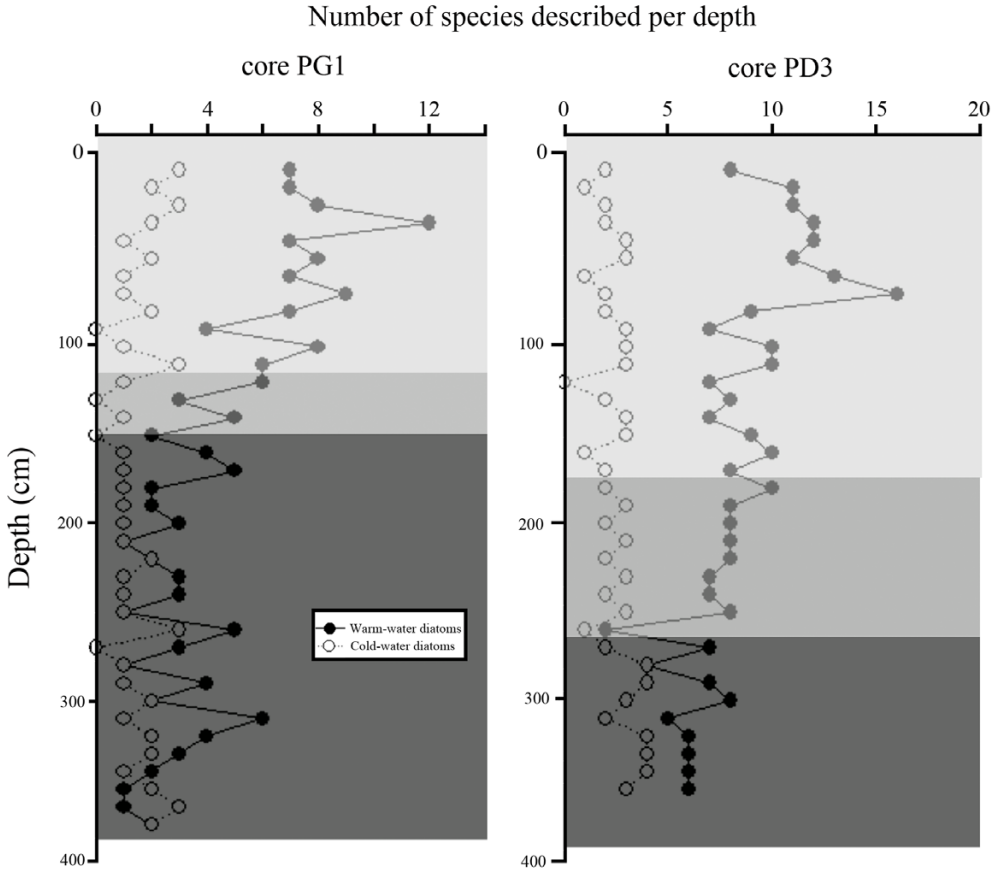

Fig. 5. Downcore changes in number of species between warm and cold water diatoms (PG1 and PD3 cores). The dark grey, grey and light grey colors represent the Late Pleistocene, Last Glacial Maximum, and Holocene zone, respectively

that the location of core PG1 was closer to land than core PD3, which would have been more influenced by freshwater. These changes also possibly resulted from the fluctuation of nutrient availability by current influx, sediment flow, and location of the collected cores. Td values suggested by Kanaya and Koizumi (1966) are adopted here to estimate surface water temperature during sediment accumulation in the lower levels of a core sequence. Fluctuation in Td values was noticed in the two cores from the Ulleung Basin, which generally increased upward in both cores (Fig. 5). No significant difference was observed before and after LGM with regard to the Td values of both cores. However, during the LGM, the Td value of PG1 was higher than that of PD3. Even if it was cold during the LGM (approximately 14.6–26.5 kyr), the number of warm-water species continuously increased (Fig. 5). During this period, warm-water species increased at 31–74 cm in core PG1 and 172–254 cm in core PD3. Cores PG1 and PD3 confirm that warm-water species (Td value) and centric species (C:P ratio) increased upward during the LGM and that geochemical factors also increased. These results indicate that the TWC continuously flowed to the East Sea. These results can also indicate the current flow in East Sea, illustrated by a high abundance of benthic or tychopelagic species and a lower abundance of planktonic species. The unstable minor fluctuations in the lower Td values corresponded to paleotemperature changes. Paleotemperature changes in the Ulleung Basin were affected by the currents in the East Sea. The Td values in the East Sea showed rhythmic fluctuations at a possible periodicity of 1,000 and 400–500 years, indicating a strong and regular flow of the Kuroshio and TWC (Koizumi 2007). Paleotemperature changes in the water environment in the Ulleung Basin are affected by the currents in the East Sea, suggesting the profound impact of paleoclimatic factors on the environment, as indicated by important changes in the populations of fossil diatoms as fundamental bioindicators.

Acknowledgments

Analyzed core samples were obtained from the Library of

Marine Samples of Korea Institute of Ocean Science and Technology (KIOST). This study was supported by a research fund from KIOST (PE99414, A Study on Ecosystem Response to Mesoscale Ocean Processes: Southern Seas of Korea), and from the Korea Ministry of Oceans and Fisheries (PM59300, Construction of test, evaluation and certification systems for USCG Phase II standard).

References

Andreen E, Andreen T, Kunzendorf H (2000) Holocene history of the Baltic Sea as a background for assessing records of human impact in the sediments of the Gotland Basin. Holocene **10**:687–702

Abrantes F (1991) Increased upwelling off Portugal during the last glaciation: diatom evidence. Mar Micropaleontol **17**(3):285–310

Battarbee RW (1986) Diatom analysis. In: Berglund BE (ed) Handbook of Holocene palaeoecology and palaeohydrology. John Wiley, Chichester, pp 527–570

Blasco D, Estrada M, Johns B (1980) Relationship between the phytoplankton distribution and composition and the hydrography in the Northwest African upwelling region near Cabo Carvoeiro. Deep-Sea Res **27**:799–821

Cooper SR (1995a) Chesapeake Bay watershed historical land use: impact on water quality and diatom communities. Ecol Appl **5**(3):703–733

Cooper SR (1995b) Diatoms in sediment cores from the mesohaline Chesapeake Bay, USA. Diatom Res **10**(1):39–89

Cha HJ, Choi MS, Lee CB, Shin DH (2007) Geochemistry of surface sediments in the southwestern East/Japan Sea. J Asian Earth Sci **29**:685–697

Flower RJ, Juggins S, Battarbee RW (1997) Matching diatom assemblages in lake sediment cores and modern surface sediment samples: the implications for conservation and restoration with special reference to acidified systems. Hydrobiologia **344**:27–40

Girard V, Saint Martin S, Saint Martin JP, Schmidt AR, Struwe S, Perrichot V, Breton G, Néraudeau D (2009) Exceptional preservation of marine diatoms in upper Albian amber. Geology **37**(1):83–86

Gebühr C, Wiltshire KH, Aberle N, van Beusekom JE, Gerdts G (2009) Influence of nutrients, temperature, light and salinity on the occurrence of *Paralia sulcata* at Helgoland Roads, North Sea. Aquat Biol **7**(3):185–197

Haschke M (2006) The Eagle III BKA system, a novel sediment core X-ray fluorescence analyser with very high spatial resolution. In: Rothwell RG (ed) New techniques in sediment core analysis. Geological Society, London, Special Publications 267, pp 31–37

Jian Z, Wang P, Saito Y, Wang J, Pflaumann U, Oba T, Cheng X (2000) Holocene variability of the Kuroshio Current in the Okinawa Trough, northwestern Pacific Ocean. Earth Planet Sc Lett **184**:305–319

Kanaya T, Koizumi I (1966) Interpretation of diatom thanatocoenoses from the North Pacific applied to a study of core V20-130 (Studies of a deep-sea core V20-130. Part IV). Sci Rep Tohoku Univ **37**:89–130

Koizumi I (2007) Climatic variations and changes in world history. J Geog **116**:62–78 (in Japanese)

Lange CB, Romero OE, Wefer G, Gabric AJ (1998) Offshore influence of coastal upwelling off Mauritania, NW Africa, as recorded by diatoms in sediment traps at 2195 m water depth. Deep-Sea Res **45**:985–1013

Lee E, Nam S (2003) Fresh-water supply by the Korean rivers to the East Sea during the last glacial maximum: a review and new evidences from the Korea Strait region. Geo-Mar Lett **23**(1):1–6

Lee E, Nam S (2004) Low sea surface salinity in the East Sea during the last glacial maximum: review on freshwater supply. Geosci J **8**(1):43–49

Lee GH, Suk BC (1998) Latest Neogene–Quaternary seismic stratigraphy of the Ulleung Basin, East Sea (Sea of Japan). Mar Geol **146**:205–224

Lim DI, Kang S, Yoo HS, Jung HS, Choi JY, Kim HN, Shin IH (2006) Late Quaternary sediments on the outer shelf of the Korea Strait and their paleoceanographic implications. Geo-Mar Lett **26**(5):287–296

Lim DI, Xu ZK, Choi JY, Kim SY, Kim EH, Kang SR, Jung HS (2011) Paleoceanographic changes in the Ulleung Basin, East (Japan) Sea, during the last 20,000 years: evidence from variations in element composition of core sediments. Prog Oceanogr **88**:101–115

Marciniak B (1981) Late-Glacial diatom phases in Western Pomerania. Acta Geol Pol **31**:127–137

Moriyasu S (1972) The Tsushima Current. In: Stommel H, Yoshida K (eds) The Kuroshio. University of Washington Press, pp 353–369

Nyagaard G (1949) Hydrobiological studies on some Danish ponds and lakes. II: the quotient hypothesis and some new or little known phytoplankton organisms. Kongel Danske Vidensk Selsk Biol Skr **7**:1–193

Oba T, Gato M, Kitazato H, Koizumi I, Omura A, Sakai T, Takayama T (1991) Paleoenvironmental changes in the Japan Sea during the last 85,000 years. Paleoceanog **6**:499–518

Park SC, Yoo DG, Lee CW, Lee EI (2000) Last glacial sea-level changes and paleogeography of the Korea (Tsushima) Strait. Geo-Mar Lett **20**(2):64–71

Pyle L, Cooper SR, Huvane JK (1998) Diatom paleoecology Pass Key Core 37, Everglades National Park, Florida Bay. US Geological Survey No. 98-522, 37 p

Reid MA, Tibby JC, Penny D, Gell PA (1995) The use of diatoms to assess past and present water quality. Aust J Ecol **20**(1):57–64

Rothwell RG, Rack FR (2006) New techniques in sediment core analysis: an introduction. In: Rothwell RG (ed) New techniques in

sediment core analysis. Geological Sociery, London, Special Publication 267, pp 1–29

Ryu E (2005) Late quaternary diatom assemblages from the Ulleung Basin, East sea. J Paleontol Soc Kor **21**(1):23–139

Ryu E, Yi S, Lee SJ (2005) Late Pleistocene–Holocene paleoenvironmental changes inferred from the diatom record of the Ulleung Basin, East Sea (Sea of Japan). Mar Micropaleontol **55**(3):157–182

Ryu E, Lee SJ, Yang DY, Kim JY (2008) Paleoenvironmental studies of the Korean peninsula inferred from diatom assemblages. Quatern Int **176**:36–45

Shannon CE, Weaver W (1949) The mathematical theory of communication. University of Illinois Press, Urbana, 117 p

Stein R, Grobe H, Wahsner M (1994) Organic carbon, carbonate, and clay mineral distributions in eastern central Arctic Ocean surface sediments. Mar Geol **119**:269–285

Schuette G, Schrader H (1979) Diatom taphocoenoses in the coastal upwelling area off western South America. Nova Hedwigia **64**:359–378

Tada R (1999) Late quaternary paleoceanography of the Japan Sea: an update. Daiyonki Kenkyu (Quat Res) **38**(3):216–222

Ujiié H, Tanaka Y, Ono T (1991) Late Quaternary paleoceanographic record from the middle Ryukyu Trench slope, northwest Pacific. Mar Micropaleontol **18**:115–128

Ujiié Y, Ujiié H, Taira A, Nakamura T, Oguri K (2003) Spatial and temporal variability of surface water in the Kuroshio source region, Pacific Ocean, over the past 21,000 years: evidence from planktonic foraminifera. Mar Micropaleontol **49**:335–364

Xu X, Oda M (1999) Surface-water evolution of the eastern East China Sea during the last 36,000 years. Mar Geol **156**:285–304

Yasuda I, Okuda K, Shimizu Y (1996) Distribution and modification of North Pacific intermediate water in the Kuroshio-Oyashio interfrontal zone. J Phys Oceanogr **26**:448–465

Yoon SH, Chough SK (1995) Regional strike-slip in the eastern continental margin of Korea and its tectonic implications for the evolution of Ulleung Basin, East Sea. Bull Geol Soc Am **107**:83–97

Witoñ E, Witkowski A (2003) Diatom (Bacillariophyceae) flora of early Holocene freshwater sediments from Skalafjord, Faeroe Islands. Micropaleontology **23**:1–26

Witkowski A (1994) Recent and fossil diatom flora of the Gulf of Gdansk, Southern Baltic Sea. Biblioth Diatomol **28**:1–313

Zong Y (1997) Implications of *Paralia sulcata* abundance in Scottish isolation basins. Diatom Res **12**:125–150

Appendix

Table 1. Ecological and biogeographical categories of diatom species

Type	Species	References
W	*Actinoptychussplendens* (Shadbolt) Ralfs in Pritchard 1861	1
W	*Asteromphaluselegans* Greville 1859	2
W	*Bacteriastrumdelicatulum* Cleve 1897	1, 3
W	*B.elegans* Pavillard 1916	2
W	*B.elongatum* Cleve 1897	1, 3
W	*B.furcatum* Shadbolt 1854	2
W	*B.hyalinum*Lauder 1864	1, 3
W	*Chaetocerosdensus* (Cleve) Cleve 1899	2
W	*C.didymus* Ehrenberg 1845	1, 3
W	*Coscinodiscuscentralis* Ehrenberg 1839	1
W	*C.nodulifer* A. Schmidt in Schmidt et al. 1878	4, 5
W	*C.perforatus* Ehrenberg 1844	4
W	*C.radiatus* Ehrenberg 1854	1, 7
W	*Cyclotellastriata*(Kützing) Grunow in Cleve & Grunow 1880	3
W	*Probosciaindica* (H. Peragallo) Hernandez-Becerril 1995	1
W	*Pseudosoleniacalcar-avis* (Schultze) B.G.Sundström 1986	3, 6
W	*Rhizosoleniabergonii* H. Peragallo 1892	3, 4, 5, 6
W	*R.formosa* H. Peragallo 1888	2
W	*R.setigera* Brightwell 1858	1
W	*Skeletonematropicum* Cleve 1900	2
W	*Thalassionemafrauenfeldii* (Grunow) Hallegraeff 1986	2
W	*Th. nitzschioides* (Grunow) Mereschkowsky 1902	3, 7, 5
W	*Thalassiosirabinata* G. Fryxell 1977	2
W	*T.mala* Takano 1965	2
W	*T.simonsenii* Hasle et G. Fryxell 1977	2
C	*Actinocycluscurvatulus* (Grunow in A. Schmidt) Cleve 1901	4, 5
C	*Asteromphalusparvulus* Karsten 1905	2
C	*Odontellaaurita* (auritum) Agardh 1832	3, 4, 5, 7
C	*Rhizosoleniahebetata* J.W. Bailey 1856	5, 6
C	*Thalassiosiranordenskioeldii* Cleve 1873	2, 3, 4, 5
C	*Thalassiothrixlongissima* Cleve & Grunow in Grunow 1880	3, 7

W: warm-water species and C: cold-water species supplemented by references. 1: Cupp (1943), 2: Hasle and Syvertsen (1996), 3: Kanaya and Koizumi (1966), 4: Koizumi (1986), 5: Koizumi (1989), 6: Koizumi (2008), 7: Ryu et al. (2005)

Appendix References

Cupp EE (1943) Marine Plankton diatoms of the west coast of North America. Bull Scripps Inst Oceanogr **5**:1–238

Hasle GR, Syvertsen EE (1996) Marine diatoms. In: Tomas CR (ed) Identifying marine phytoplanktion. Academic Press, San Diego, pp 5–385

Kanaya T, Koizumi I (1966) Interpretation of diatom thanatocoenoses from the North Pacific applied to a study of core V20-130 (Studies of a deep-sea core V20-130. Part IV). Sci Rep Tohoku Univ Ser 2 (Geol) **37**:89–130

Koizumi I (1986) Pliocene and Pleistocene diatom datum levels related with paleoceanography in the northwest Pacific. Mar Micropaleontol **10**(4):309–325

Koizumi I (1989) Holocene pulses of diatom growths in the warm Tsushima Current in the Japan Sea. Diatom Res **4**:55–68

Koizumi I (2008) Diatom-derived SSTs (Td′ ratio) indicate warm seas off Japan during the middle Holocene (8.2–3.3 kyr BP). Mar Micropaleontol **69**(3):263–281

Ryu E, Yi S, Lee SJ (2005) Late Pleistocene–Holocene paleoenvironmental changes inferred from the diatom record of the Ulleung Basin, East Sea (Sea of Japan). Mar Micropaleontol **55**(3):157–182

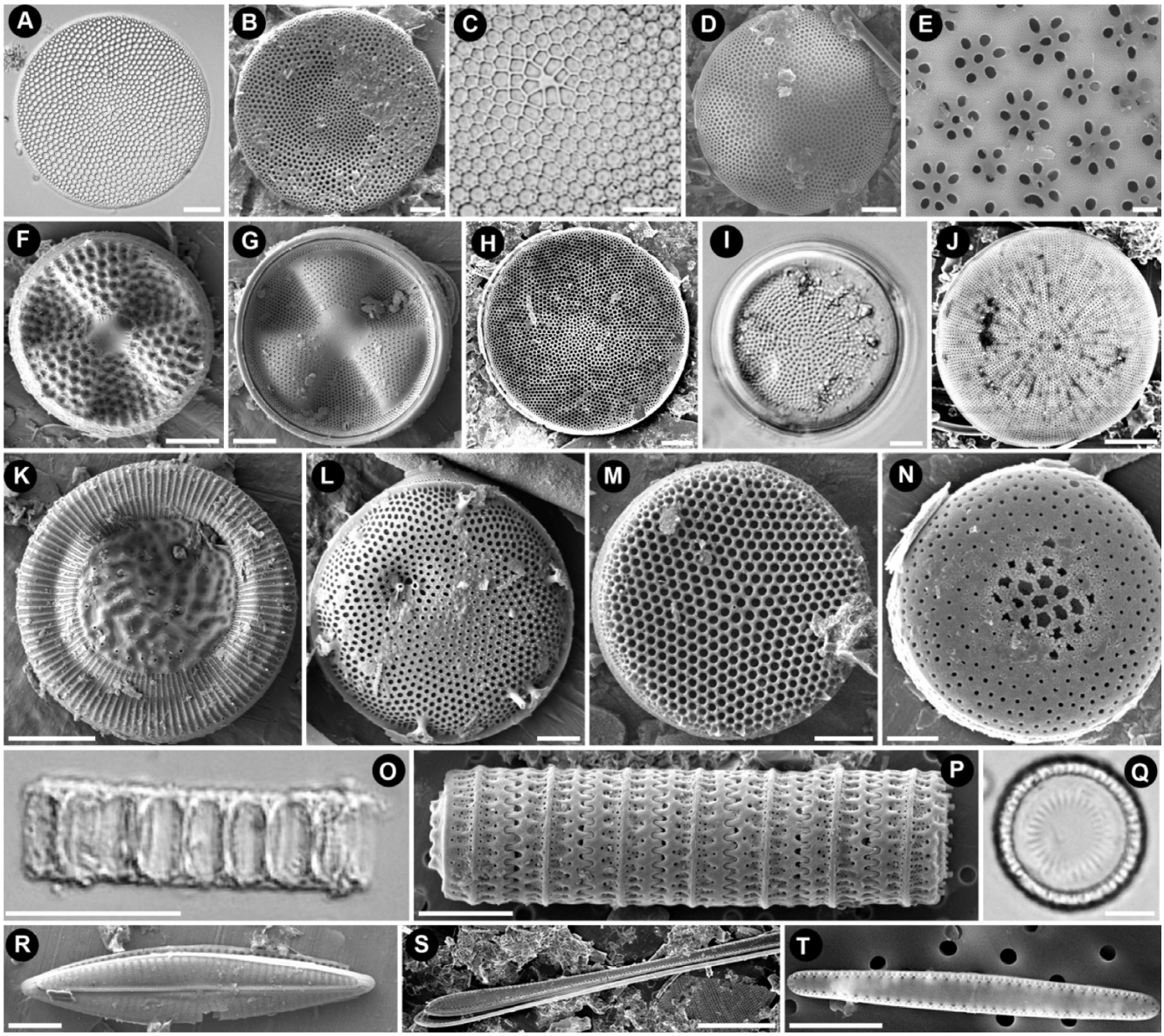

Plate 1. PG1 and PD3 fossil diatom. Figs A-C. *Coscinodiscus asteromphalus*; Figs D–E. *C. centralis*; Figs F-G. *Actinoptychus senarius*; Fig. H. *Actinocyclus curvatulus*; Figs I-J. *A. octonarius*; Fig. K. *Cyclotella* sp.; Fig. L. *Thalassiosira curviseriata*; Fig. M. *T. eccentrica*; Fig. N. *T. mala*; Figs O-Q. *Paralia sulcata*; Fig. R. *Navicula* sp.; Fig. S. *Thalassionema faruenfeldii*; Fig. T. *Th. Nitzschioides.* Scale bars = 1 μm (Fig. E); 2 μm (Fig. L); 5 μm (Figs G, M, Q, R); 10 μm (Figs C, F, H, J, K, N, O, S, T); 20 μm (Figs A, B, D, I); 30 μm (Figs. P). Figs A, C, I, O, Q: LM. Figs B, D-H, J-N, P, R-T: SEM